# Multi-carrier synthetic aperture communication in shallow water: Experimental results

Taehyuk Kang,[a] H. C. Song, and W. S. Hodgkiss
*Marine Physical Laboratory, Scripps Institution of Oceanography, University of California, San Diego, La Jolla, CA 92093-0238*

(Received 22 November 2010; revised 23 August 2011; accepted 16 September 2011)

Orthogonal frequency division multiplexing (OFDM) communications in the presence of motion is investigated using data collected from the Kauai Acomms MURI 2008 (KAM08) experiment, conducted off the western side of Kauai, Hawaii, in June–July 2008. The experiment involved a vertical array moored in 106 m deep shallow water and a source towed at a speed of 3 knots at ranges between 600 m and 6 km. In order to attain reliable communications with only a single receive element, a synthetic aperture approach is applied. After combining multiple transmissions, an error-free reception is achieved with a low-density parity-check code, confirming the feasibility of coherent synthetic aperture communications using OFDM. © *2011 Acoustical Society of America*. [DOI: 10.1121/1.3652855]

PACS number(s): 43.60.Dh, 43.60.Gk, 43.60.Fg [WMC] Pages: 3797–3802

## I. INTRODUCTION

The main advantage of orthogonal frequency division multiplexing (OFDM) is its ability to cope with channels with large delay spread without complex equalizers. In addition, time-varying channels easily can be dealt with by updating the channels on a block-by-block basis. In terrestrial communications, OFDM has become a favorite choice for many wireless communications such as Digital Audio/Video Broadcasting, wireless LAN (local area network), and next-generation of cellular networks. Also, OFDM has attracted attention recently in underwater acoustic communications (UAC) due to its robustness in dispersive channels. Examples of OFDM applications to UAC can be found in Refs. 1–6 while the OFDM algorithm itself is well documented in the wireless literature.[7]

However, OFDM is known to be sensitive to Doppler effects because Doppler introduces intercarrier interference (ICI) and destroys the orthogonality of the subchannels. Due to the low sound speed (1.5 km/s) in underwater channels, even a small movement can introduce a significant Doppler shift. The Doppler can be time-varying and the temporal variability of the channel induces Doppler spreading. In addition, underwater acoustic communication signals frequently are wideband with bandwidths exceeding 20%–30% of the carrier frequency. Thus, wideband OFDM introduces a nonuniform Doppler shift across the subcarriers in the presence of motion.[3] Few algorithms are reported in the literature to mitigate the Doppler effects in underwater OFDM applications. Tu *et al.*[2] proposed a frequency domain decision feedback equalizer (FD-DFE) to deal with Doppler spread. Li *et al.*[3] applied a two-step approach (resampling and residual offset correction) to compensate for a Doppler shift and showed experimental results involving a mobile platform.

In underwater acoustic communications, a vertical array can be employed (spatial diversity) to enhance signal to noise ratio (SNR) and mitigate channel fading effects. Similarly, synthetic aperture communication (SAC)[8] can be utilized where spatial diversity is obtained from a virtual horizontal array generated by relative motion between a single transmitter and a single receiver. Originally the term "synthetic aperture" is used for radars which exploit the relative motion to achieve finer spatial resolution. However the SAC approach adopted here for communications and in Ref. 8 is not to increase the spatial aperture (or resolution), but to achieve spatial/temporal diversity. In this paper, we use at-sea experimental data to demonstrate that the SAC approach can be applied to underwater OFDM communications in a moving source scenario. Diversity combining not only increases SNR but also mitigates ICI, which is an additional benefit especially for OFDM transmissions as reported in Refs. 9 and 10.

The paper is organized as follows. Section II describes the Kauai Acomms MURI 2008 (KAM08) source-tow experiment and then OFDM signal design and receiver algorithm. Performance analysis is presented in Sec. III, followed by a summary in Sec. IV.

## II. EXPERIMENTAL DETAILS

### A. System setup

The KAM08 source-tow experiment data analyzed in this paper was collected off the western side of Kauai, Hawaii, on July 1 (JD 183) 2008. A schematic of the experiment is shown in Fig. 1. A vertical receive array (VRA) was moored in 106 m deep water. The VRA consisted of 16-elements spanning a 56.25 m aperture with 3.75 m element spacing, covering about half the water column. The sampling rate at the receiver was 50 kHz and a bandwidth of 8 kHz (12 – 20 kHz) is selected for data communication based on the source characteristics (ITC-1001 with a resonant peak at 16.5 kHz).

[a]Author to whom correspondence should be addressed. Electronic mail: tedkang@ucsd.edu

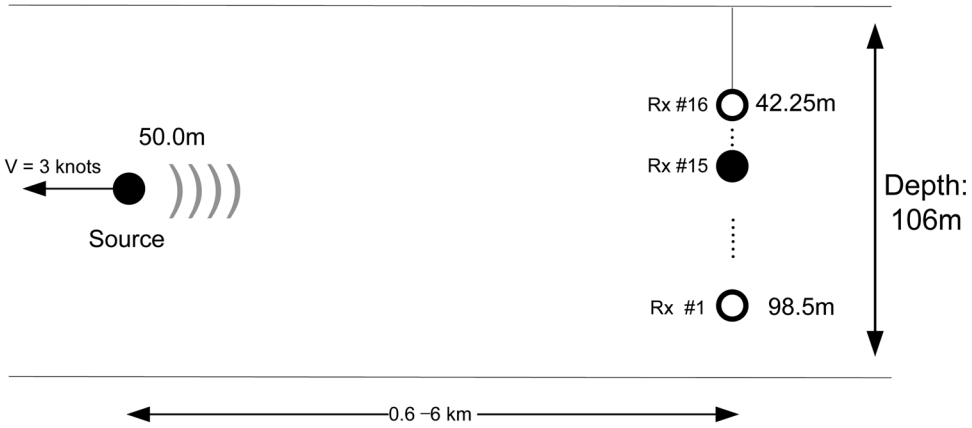


FIG. 1. Schematic of the KAM08 experiment. A vertical receive array (VRA) was moored in 106 m deep water. The VRA consisted of 16-elements spanning a 56.25 m aperture with 3.75 m element spacing. A single source is deployed to 50 m depth and towed by the R/V Melville at 3 knots.

A single source was towed at a speed of 3 knots (1.5 m/s) and depth of 50 m by R/V Melville.

The trajectory of the ship towing the source is shown in Fig. 2. The source tow started at 00:00 coordinated universal time (UTC) from the start point (x) and proceeded along the waypoints in a clockwise direction for about four hours. The identical OFDM packets were transmitted every 15 minutes, for a total of 16 times from 00:11 to 03:56 UTC. The OFDM transmissions are denoted by Tx # such that Tx #1 is the first OFDM signal transmitted at 00:11, Tx #2 is at 00:26, …, #16 is at 03:56. The shortest distance between the source and the VRA was 600 m at 02:11 UTC (Tx #9) and the longest distance was 6 km at 01:11 UTC (Tx #5).

Since we are interested in SAC, a single element will be selected from the VRA and multiple transmissions will be combined.

## B. Signal design

### 1. Packet design

The OFDM data packet structure is illustrated in Fig. 3. Each packet consists of a 100 ms long linear frequency modulated (LFM) waveform, 100 ms silence period, followed by eight OFDM blocks with each block being 148 ms long. The total packet duration is 1.384 second. The LFM waveform at the beginning of the packet is used for synchronization and Doppler shift estimation.

### 2. OFDM design

A block diagram for the transmitter is shown in Fig. 4(a). First, an information bit sequence is low-density parity-check (LDPC) coded.[11,12] The sequence then is mapped into symbols using quadrature phase shift keying (QPSK). The OFDM modulator in Fig. 4(a) consists of a serial to parallel converter, inverse fast Fourier transform (IFFT), cyclic prefix adder, and upconverter.

The OFDM system specifications are listed in Table I. Each OFDM block contains 672 information bits or 1344 LDPC coded bits (one codeword). The pilots are equally spaced at every fourth subcarrier. The cyclic prefix (CP) length is set to 20 ms and the multipath arrivals after the CP length are treated as additive noise at the receiver. The number of subcarriers is chosen such that the subcarrier bandwidth is much less than the coherence bandwidth (the bandwidth where the channel frequency response is relatively flat) and

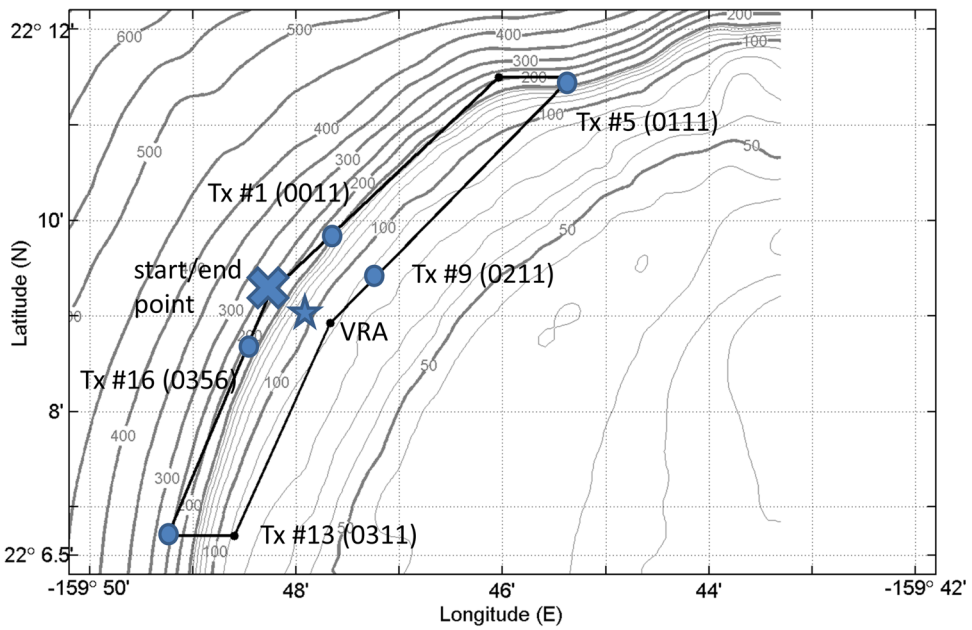


FIG. 2. (Color online) Ship trajectory during the KAM08 experiment. The source tow started at 00:00 UTC from the start point (x) and proceeded along the waypoint in a clockwise direction. The identical OFDM packets were transmitted every 15 minutes, a total of 16 times from 00:11 to 03:56 UTC. The shortest distance between a transmitter and the vertical receive array (VRA denoted by ★) was 600 m at 02:11 UTC (Tx #9) while the longest distance was about 6 km at 01:11 UTC (Tx #5).

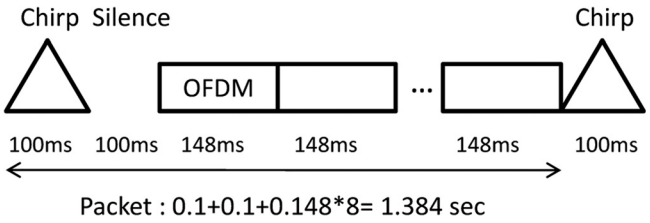


FIG. 3. OFDM packet structure. A packet consists of a 100 ms long Linear Frequency Modulated (LFM) waveform and 100 ms silence period followed by 8 OFDM blocks. The total packet duration is 1.384 second.

larger than Doppler spread of the channel. Therefore, the OFDM waveform design in the experiment (Table I) can handle a channel with up to 20 ms of delay spread and a channel without significant variation over 148 ms.

### C. Receiver algorithm

A block diagram for the receiver is shown in Fig. 4(b). The OFDM demodulator in Fig. 4(b) consists of a down-converter, cyclic prefix remover, and FFT. More details about the conventional OFDM demodulator can be found in Ref. 7. In this section, we review the algorithms of Doppler compensation, channel estimation, and diversity combining in detail.

#### 1. Synchronization and Doppler compensation

A synchronization process at each transmission is done by matched filtering of the LFM waveform at the beginning of the data transmission.

For Doppler compensation, we assume that change in Doppler shift is minimal within the packet duration, which is a reasonable assumption for our packet design (1.384 second). Doppler compensation is done as follows. First, the receiver correlates two channel responses obtained from the LFM probes (one at the beginning of the packet and the other at the beginning of the next packet). Then, the receiver finds the peak of the correlation and estimates the time duration of the received packet ($\hat{T}$). Third, the Doppler scale factor ($\beta$) is estimated by comparing the designed packet duration ($T$) with the received packet duration ($\beta = (\hat{T} - T)/T$). Finally, the received waveform is resampled according to the estimated Doppler. A similar Doppler estimation algorithm is introduced in Ref. 3, where the time duration of the received packet is

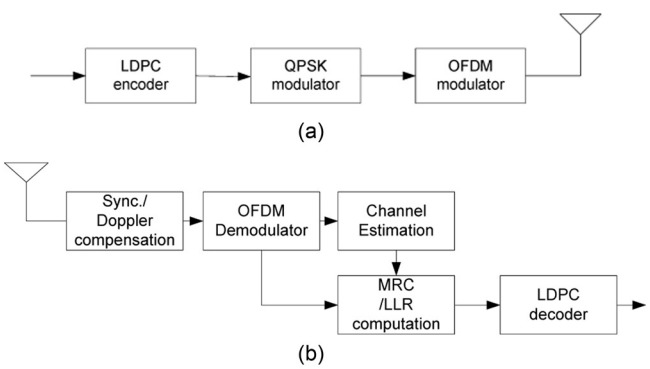


FIG. 4. Block diagrams: (a) Transmitter and (b) receiver.

TABLE I. OFDM system specifications.

| | |
|---|---|
| FFT size ($N_s$) | 1024 |
| Number of Data subcarriers | 672 |
| Number of pilots | 230 |
| Bandwidth | 8 kHz (12 – 20 kHz) |
| Subcarrier BW | 7.81 Hz |
| Cyclic prefix duration | 20 ms |
| Symbol duration including CP | 148 ms |
| Uncoded Data rate (QPSK) | 9181 bps |
| Uncoded spectral efficiency (QPSK) | 1.15 bits/s/Hz |
| Coded Data rate (QPSK) | 4541 bps |
| Coded spectral efficiency (QPSK) | 0.57 bits/s/Hz |
| LDPC decoder | (1344,672) half-rate IEEE 802.16e |

estimated from independent synchronization processes of two adjacent packets. The packet is synchronized based on the strongest tap of the channels.

#### 2. Channel estimation and diversity combining

Channel estimation is carried out using pilot symbols on a block-by-block basis. Given the channel estimates at the pilot sub carriers, the channels at all other subcarriers are estimated by orthogonal matching pursuit (OMP). The underwater channel often exhibits sparse characteristics (see Fig. 5), where the channel has a large delay spread but many of the channel taps have negligible values.[6] The OMP algorithm is used in the analysis since it is shown to yield accurate estimates for a sparse channel.[1]

Diversity combining is achieved by maximal ratio combining (MRC). Since OFDM decomposes an intersymbol interference (ISI) channel into non-ISI sub-channels, MRC easily can be applied to each data subcarrier in the frequency domain. Let the received signal and the channel in the frequency domain be $y_{n,k}$ and $h_{n,k}$ at the $n$th transmission and $k$th subcarrier. Then $y_{n,k}$ is modeled as

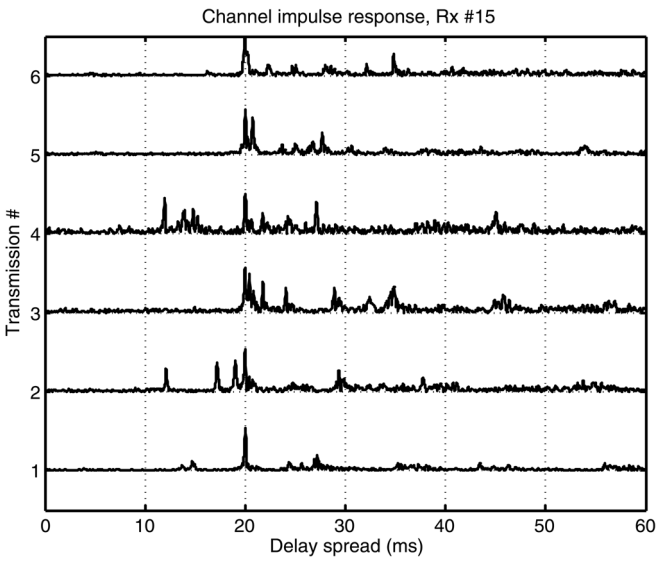


FIG. 5. Channel impulse responses (envelope) at 46 m depth (Rx #15) for six consecutive transmissions. The strongest paths are aligned at 20 ms.

$$y_{n,k} = h_{m,k}S_k + w_{n,k}, \tag{1}$$

where $s_k$ is the data symbol at subcarrier $k$ and $w_{n,k}$ is additive Gaussian noise with variance of $\sigma^2$. The MRC output at subcarrier $k$ is given by $r_k = \sum_n a_{n,k}y_{n,k}$ where $\alpha_k = h^*_{n,k}/\sum_n |h_{n,k}|^2$ and * denotes complex conjugate. The log-likelihood ratio (LLR) of the first coded bit ($c_{k,1}$) of the symbol at subcarrier $k$ is computed as

$$LLR(c_{k,1}) = \log\frac{P(c_{k,1}=1)}{P(c_{k,1}=0)} = 2\frac{\mathrm{Re}(r_k)}{\sigma^2}, \tag{2}$$

and similarly for $c_{k,2}\big(LLR(c_{k,2}) = 2(\mathrm{Im}(r_k)/\sigma^2)\big)$, which will be the input to the LDPC decoder.

Even though the Doppler shift is compensated by resampling as discussed in Sec. II C 1, there still may be residual Doppler spread causing ICI due to the time-varying channel. Although not optimum, it is shown that MRC can reduce ICI providing considerable performance improvement due to the fact that the ICIs are incoherently combined.[9,10,13]

## III. PERFORMANCE ANALYSIS

The performance analysis in this section is mainly based on the signal at Rx #15 (at a depth of 46 m). However, the other receivers show similar results.

### A. Channel characteristics

An example of the channel impulse responses (CIRs) using the LFM probe is shown in Fig. 5 for the Rx #15 during the first six transmissions. Note that the CIRs are quite different from each due to them being estimated at different times and ranges. Most of the transmissions show a delay spread less than 20 ms (CP length). When the delay spread exceeds the CP length, however, the arrivals beyond the CP will be treated as noise.

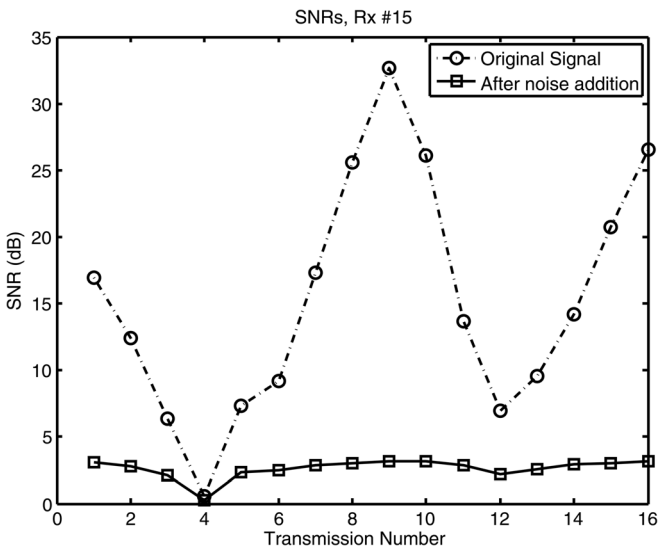


FIG. 6. Signal to noise ratios (SNRs) at Rx #15 along the transmission sequences. The estimated SNRs vary from 1 dB to 32 dB depending on the distance between the transmitter and the receiver.

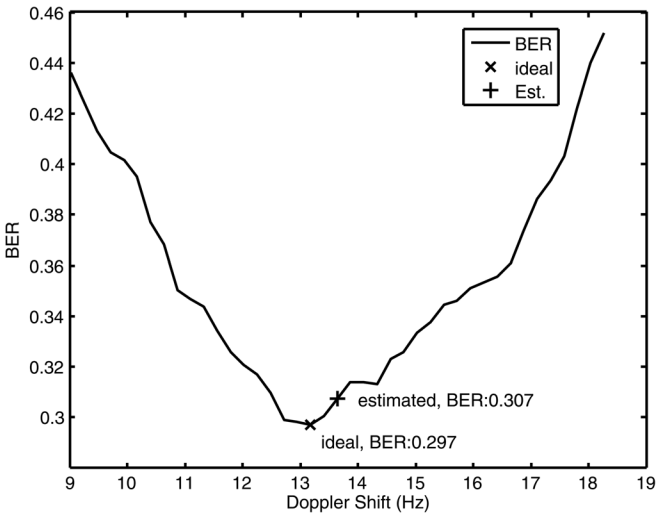


FIG. 7. Performance of Doppler shift estimation at Rx #15. The horizontal axis is the induced Doppler shift at the center frequency (16 kHz). The plot is the BER after resampling with the corresponding Doppler shift. The "+" symbol is the estimated Doppler shift. The difference of the Doppler shift between the estimate and "×" symbol is about 0.4 Hz or about 5.1% of subcarrier spacing. The corresponding BER difference is negligible.

The estimated SNRs in Fig. 6, (○) show significant variability from 1 dB to 32 dB depending on the distance between the source and receiver. To demonstrate the SAC approach in this paper, we add ambient noise recorded separately during the experiment to the individual receptions in order to lower the input SNR to approximately 3 dB. Note that Tx #4 whose SNR is below the target SNR will be excluded from the processing. These modifications reflect a more realistic scenario where the range separation between transmissions would be much shorter[8] (e.g., a few 10 s of m) so that the SNRs would not change significantly while still providing sufficient diversity. The estimated SNRs after noise addition (□) are shown in Fig. 6.

### B. Doppler compensation

To assess the accuracy of the Doppler estimation, the bit error rate (BER) performance for Tx #2 is displayed in

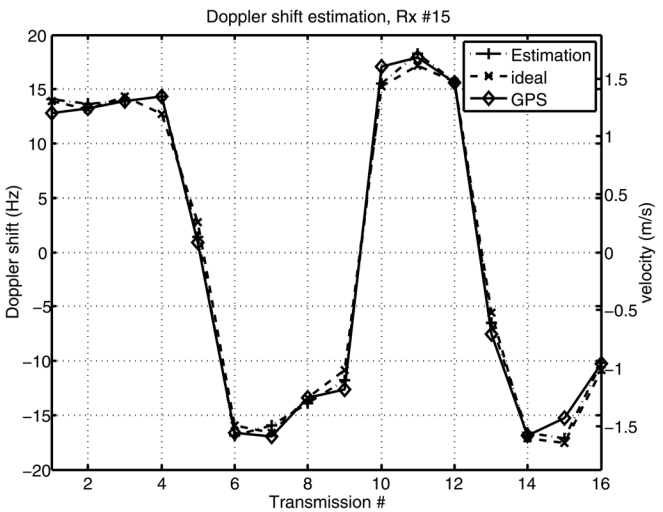


FIG. 8. Doppler estimations along the transmission sequences. The right vertical axis indicates the corresponding relative velocity.

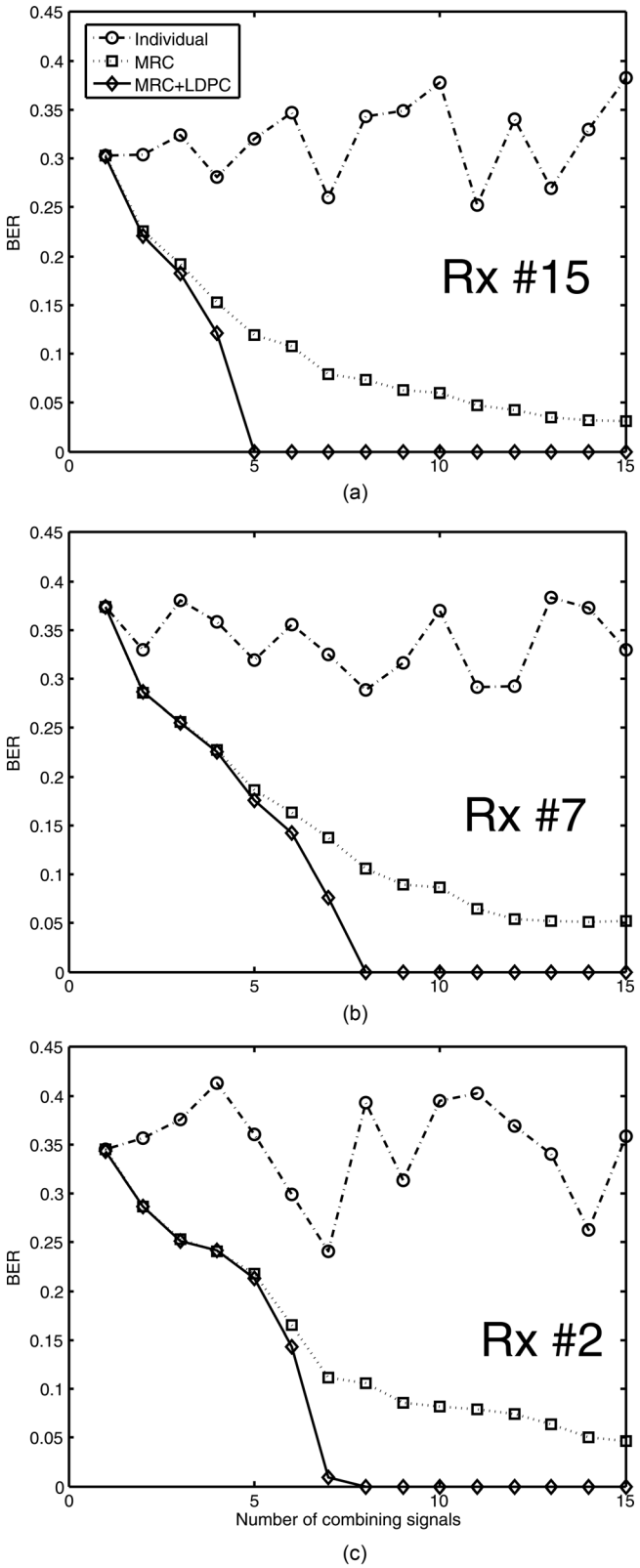


FIG. 9. Performance comparison (a) top (Rx #15), (b) middle (Rx #7), (c) bottom (Rx #2). Three different approaches are compared: (1) Individual performance without combining (○), (2) MRC without coding (□), and (3) MRC with LDPC decoding (◊).

Fig. 7 as a function of a Doppler shift at the center frequency of 16 kHz. The best performance is obtained at a Doppler shift of 13.2 Hz (×). The curve sharply rises as it deviates from the minimum (×), showing that OFDM is very sensitive to Doppler. For comparison purposes, the "+" symbol denotes the estimated Doppler shift (13.6 Hz) from the algorithm described in Sec. II C. The difference between the two is about 0.4 Hz or about 5.1% of the subcarrier spacing (7.81 Hz), indicating that the estimation algorithm provides a reasonable Doppler shift estimate.

Now the estimated Doppler shifts (+) are shown in Fig. 8 for all 16 transmissions while the Doppler shifts offering the best performance (x) are superimposed as "ideal." In addition, the global positioning system (GPS)-derived Doppler shift (◊) is calculated from the actual GPS and ship heading data. Not surprisingly, a wide range of Doppler shifts are shown between −15 Hz and 15 Hz due to the ship trajectory in our experimental setup. The "+" and "×" curves match very well within 0.5 Hz, confirming the validity of the Doppler extimation/compensation algorithm proposed.

### C. Performances

To investigate the impact of SAC diversity combining on performance, BERs of Rx # 15 are shown in Fig. 9(a) as a function of the number of transmissions combined. Three different approaches are compared: (1) Individual performance without combining (○), (2) MRC without coding (□), and (3) MRC with LDPC decoding (◊).

First, the BERs without combining (○) are quite high (25%–38%) due to a combination of low SNR (3 dB) and/or residual Doppler effects. Second, generally the performance improves with an increase in diversity. Once the "MRC" curve (□) reaches a BER about less than 10%, we obtain error-free reception (◊). This phenomenon can be attributed to the threshold characteristics of the LDPC code. Once the quality of the signal is better than a certain level, a slight improvement in input results in significant performance enhancement. Finally, error-free reception is achieved by five transmissions with coding.

To check the consistency of the results, the performances of Rx #7 (at a depth of 64.75 m, middle) and #2 (at a depth of 94.75 m, near bottom) are also plotted in Fig. 9(b) and Fig. 9(c), respectively. Even though not shown here, other receivers at different depths achieve error-free performance after combining between five and eight transmissions.

In the experiment, we transmitted identical sequences every 15 minutes. However, in practice, the period of the transmission can be shortened as long as the channels at each transmission are fairly independent so that the spatial and temporal diversity can be exploited.

## IV. CONCLUSION

In this paper, the OFDM signaling scheme was extended to synthetic aperture communications exploiting the relative motion between a source and a receiver. The KAM08 experiment data analyzed was from a single source towed at 3 knots and a vertical receiver array over various distances (0.6 – 6 km) using an 8 kHz bandwidth (12 – 20 kHz). Error-free receptions were demonstrated after multiple transmission combining and LDPC decoding, confirming successful implementation of OFDM-based synthetic aperture communications in shallow water.

## ACKNOWLEDGMENTS

This work was supported by the Office of Naval Research under Grant No. N00014-07-1-0739. The authors are grateful to Paul Hursky (Heat, Light, & Sound Research, Inc.) and Tolga Duman (Arizona State University) for designing the OFDM waveforms transmitted during the KAM08.

[1]T. Kang and R. Iltis, "Iterative carrier frequency offset and channel estimation for underwater acoustic OFDM systems," IEEE J. Sel. Areas Commun. **26**, 1650–1661 (2008).

[2]K. Tu, D. Fertonani, T. Duman, and P. Hursky, "Mitigation of intercarrier interference in OFDM systems over underwater acoustic channels," in *Proc. MTS/IEEE OCEANS* (2009), Vol. 1.

[3]B. Li, S. Zhou, M. Stojanovic, L. Freitag, and P. Willett, "Multicarrier communication over underwater acoustic channels with nonuniform Doppler shifts," IEEE J. Ocean. Eng. **33**, 198–209 (2008).

[4]S. Mason, C. Berger, S. Zhou, and P. Willett, "Detection, synchronization, and Doppler scale estimation with multicarrier waveforms in underwater acoustic communication," IEEE J. Sel. Areas Commun. **26**, 1638–1649 (2008).

[5]T. Kang, H. Song, W. Hodgkiss, and J. Kim, "Long-range multi-carrier acoustic communications in shallow water based on iterative sparse channel estimation," J. Acoust. Soc. Am. **128**, EL372–EL377 (2010).

[6]C. Berger, S. Zhou, J. Preisig, and P. Willett, "Sparse channel estimation for multicarrier underwater acoustic communication: From subspace methods to compressed sensing," IEEE Trans. Signal Process. **58**, 1708–1721 (2010).

[7]A. Bahai and B. Saltzberg, *Multi-Carrier Digital Communications: Theory and Applications of OFDM*, 2nd ed. (Springer, New York, 2004), pp. 1–436.

[8]H. C. Song, W. S. Hodgkiss, W. A. Kuperman, T. Akal, and M. Stevenson, "High-rate synthetic aperture communications in shallow water," J. Acoust. Soc. Am. **126**, 3057–3061 (2009).

[9]J. Rinne, "Subcarrier-based selection diversity reception of DVB-T in a mobile environment," in *Proc. IEEE Vehicular Technology Conf. (VTC)* (2002), Vol. 2, pp. 1043–1047.

[10]M. Russell and G. Stuber, "Interchannel interference analysis of OFDM in a mobile environment," in *Proc. IEEE Vehicular Technology Conf. (VTC)* (1995), Vol. 2, pp. 820–824.

[11]R. Gallager, "Low-density parity-check codes," IEEE Trans. Inf. Theory **8**, 21–28 (1962).

[12]D. MacKay, "Good error-correcting codes based on very sparse matrices," IEEE Trans. Inf. Theory **45**, 399–431 (1999).

[13]A. Hutter, E. de Carvalho, J. Cioffi, "On the impact of channel estimation for multiple antenna diversity reception in mobile OFDM systems," in *Proc. IEEE Asilomar Conf. on Signals, Systems and Computers (ACSSC)* (2002), Vol. 2, pp. 1820–1824.